
Dealloying of electrodeposited zinc–nickel alloy coatings

Emilija Ivaškevič,
Algirdas Selskis,
Aloyzas Sudavičius and
Rimantas Ramanauskas

*Institute of Chemistry,
A. Goštauto 9,
LT-2600, Vilnius, Lithuania*

The selective dissolution of electrodeposited Zn–Ni alloy in NaCl, NaHCO₃ and (NH₄)₂SO₄ solutions was investigated at the open circuit and in the anodic potential regions. The highest values of the dissolution selectivity factor for polarized electrodes were determined in (NH₄)₂SO₄, while the lowest in NaHCO₃ media. The selective corrosion of Zn–Ni alloy is accompanied by formation of a Ni-enriched surface layer, causing a decrease of the anodic Tafel constants in the case of electrode polarization in NaCl solution, and an increase of the diffraction line integral breadth values, implying formation of a more distorted metal lattice. The corrosion product – a film formed on Zn–Ni surface in NaCl solution – was found to be thicker than the film formed in NaHCO₃ media.

Key words: Zn–Ni alloy coatings, corrosion, selective dissolution

INTRODUCTION

Electrodeposited Zn alloys with Fe group metals extend significantly the steel corrosion protection period as compared to conventional Zn coatings. The most outstanding resistance during an atmospheric corrosion test among Zn, Zn–Co, Zn–Fe and Zn–Ni samples was detected for the latter one [1]. Hence, Zn–Ni coatings can expect a wide application, especially in car industry.

Several hypotheses have been advanced to explain the beneficial influence of alloying of Zn coatings, assuming that corrosion inhibition may be related to the structural and electronic properties of a passive oxide film, which forms the inner layer of the corrosion products [2, 3]. Furthermore, it was revealed [4] that the alloy structure, specifically the number of lattice imperfections, may be responsible for the oxide film properties, which determine the coatings corrosion resistance. A disordered lattice of Zn–Ni coating makes a bare surface more active for oxide layer formation and at the same time determines the properties of the oxide film. The amorphous structure and a higher content of hydrated Zn oxide in the film make Zn–Ni coating more resistant as compared to pure Zn and the other mentioned alloys.

The loss of the alloy properties often occurs by de-alloying, *i.e.* selective dissolution of the less noble metal. Some selective corrosion of Zn may occur for electrodeposited Zn–Ni coatings [5–9], resulting

in a certain layer enrichment with the kinetically slower component, and it may act as an improved barrier layer in the alloy corrosion process [10, 11].

The current study is part of an ongoing investigation aimed at understanding the higher corrosion resistance of Zn–Ni alloy as compared to pure Zn coatings. The present study was intended to investigate the details of Zn–Ni alloy selective dissolution and the role of this phenomenon in the corrosion behaviour of this electrodeposit.

EXPERIMENTAL

Zn and Zn–Ni (12%) coatings 10 μm thick were electrodeposited on low carbon steel samples, which had been previously polished mechanically to a bright mirror. Alkaline cyanide-free plating solutions contained ZnO 10 g l⁻¹, NaOH 100 g l⁻¹, organic additives, and ions of alloying elements. The plating bath composition and operating conditions have been presented elsewhere [12, 13].

XPS spectra were obtained with an ESCALAB MK spectrometer. The X-ray source was operated using Mg K_α (1253.6 eV, pass energy 20 eV) radiation. Surface cleaning during measurements was carried out by Ar⁺ sputtering at 15 kV accelerating voltage and beam current of 20 μA cm⁻².

An X-ray diffractometer with a grazing incident geometry (Siemens, model D 5000), Cu monochromatic radiation λ = 1.5406 Å (35 mA and 40 kV) with a 0.01° step and 4.8 s per step counter time

was used to determine the coating texture and to identify the composition of the corrosion product films. The X-ray incidence angle was 10° .

An JEOL 35C with the energy dispersive X-ray analysis (EDXA, Unispec System 700) was applied for determination of the local concentration of elements on the corroded samples.

Chemical composition analysis of coatings was performed with a Beckman Spectraspan VI direct current plasma emission spectrometer. The following spectral lines were used: 206.200 nm (Zn) and 243.789 nm (Ni).

All electrochemical measurements were made using a standard three-electrode system with a Pt counter electrode, an Ag/AgCl reference electrode and an Achema potentiostat including the Master software. The selective dissolution of Zn-Ni alloy electrodeposits was studied in 0.1 M NaCl, 0.1 M NaHCO₃ and 0.1 M (NH₄)₂SO₄ solutions at the corrosion potential and in the anodic polarization region.

RESULTS AND DISCUSSION

Polarization measurements

Polarization curves for binary alloys in an aggressive aqueous environment in general exhibit a region of a very low potential-independent current (a), followed by another region of a rapidly increasing current (b) [14]. Hence, the potential transition between regions takes place at E_c , the critical potential of the alloy.

According to the literature data, active dissolution of Zn and Zn alloys takes place in 1 M (NH₄)₂SO₄ solution [15], while corrosion in nearly neutral Cl⁻ media occurs with the formation of oxide/hydroxide film. If the medium is unbuffered (NaCl), the formed film is somewhat porous [16], while in a HCO₃⁻-containing solution the oxide film is supposed to be of a passivating character [17]. In order to evaluate the influence of the film on the dealloying process these three different media were applied. The obtained polarization curves are presented in Fig. 1. The shortest region (a) and the most negative values of the E_c (-1.0 V, Ag/AgCl) were detected for Zn-Ni alloy in a (NH₄)₂SO₄ solution. On the contrary, the most positive E_c (-0.570 V, Ag/AgCl) was detected in a passivating NaHCO₃ solution. E_c in NaCl medium was somewhat in between the two previous cases ($E_c \sim -0.770$ V, Ag/AgCl). It can be stated therefore that polarization curves of Zn-Ni alloy in all investigated solutions are typical for the metal dealloying case.

The anodic dissolution of Zn-Ni alloy, as has been detected by Baldwin et al. [18], leads to chan-

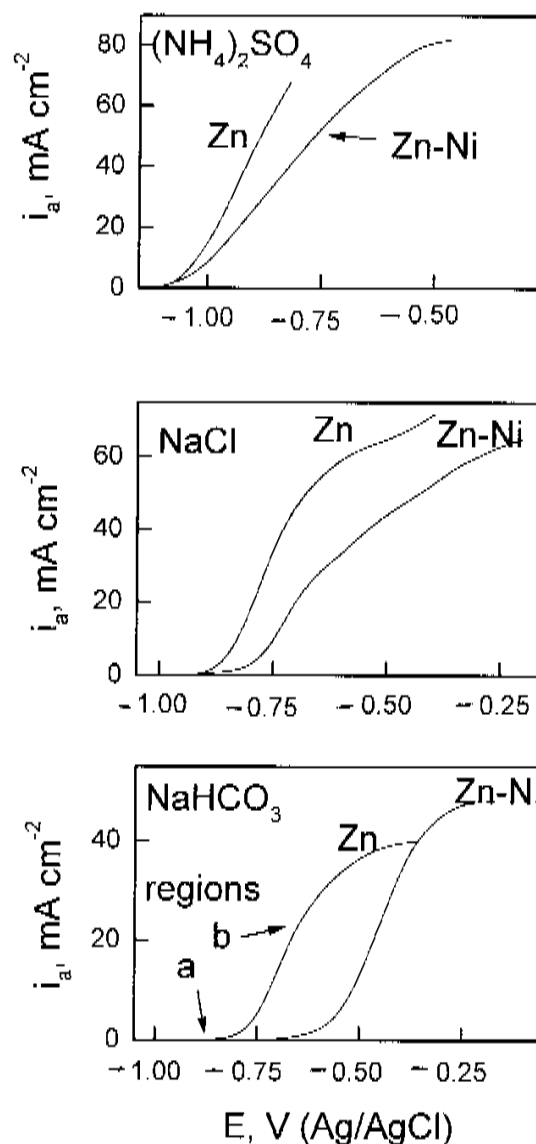


Fig. 1. Anodic polarization of Zn, Ni and Zn-Ni electrodes in (NH₄)₂SO₄ (pH 6.0), NaCl (pH 6.0) and NaHCO₃ (pH 8.4) aqueous solutions. Potential sweep rate 2 mV s⁻¹

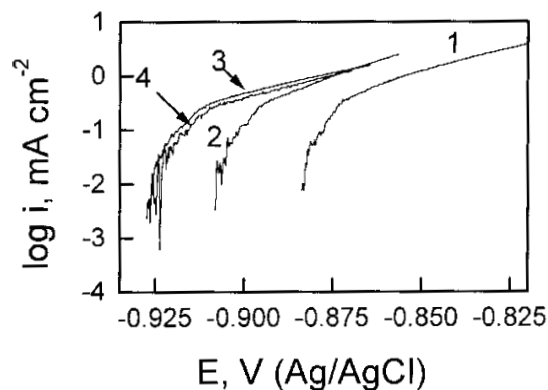


Fig. 2. Anodic polarization curves of Zn-Ni electrode in 0.1 M NaCl solution with previous immersion in NaCl test media. Immersion time (h): 1 - 0, 2 - 24, 3 - 48, 4 - 72. Scan rate 0.1 mV s⁻¹

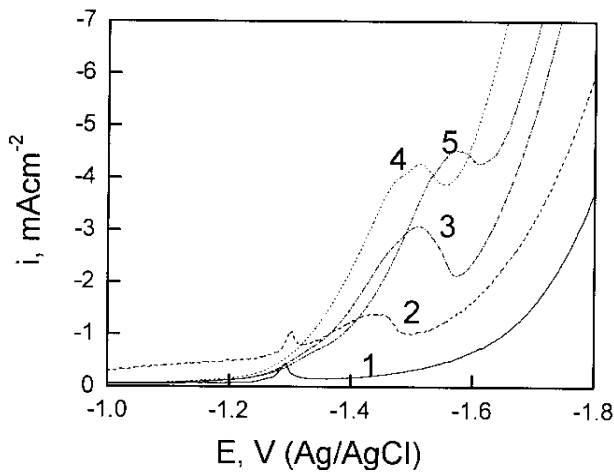


Fig. 3 Cathodic polarization curves of Zn–Ni electrode after different time of immersion in NaCl solution (h): 1 – 0; 2 – 12; 3 – 24; 4 – 48; 5 – 72. Sweep rate 2 mV s⁻¹

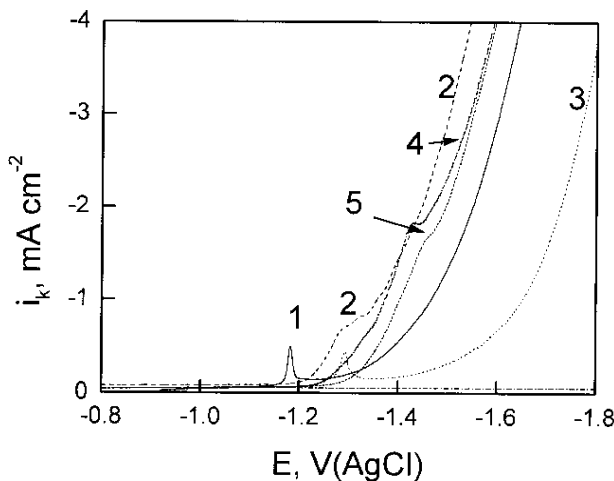


Fig. 4. Cathodic polarization curves of Zn–Ni electrode after different time of immersion in NaHCO₃ solution (h): 1 – 0; 2 – 12; 3 – 24; 4 – 48; 5 – 72. Sweep rate 2 mV s⁻¹

ges in the anodic Tafel constants. Figure 2 depicts anodic polarization curves of Zn–Ni alloy after different periods of corrosion attack. This parameter is required to obtain corrosion current values from the polarization resistance measurements. A slight decrease in β_a values for the higher immersion time can be stated, as it changes from 23.5 mV dec⁻¹ for a freshly prepared sample up to 15.3 mV dec⁻¹ for a sample exposed for 72 h to NaCl solution. This

implies that the surface of the alloy changes, what is possibly related to selective dissolution.

Corrosion of Zn and Zn alloys in a nearly neutral solution occurs with the oxide phase formation on the metal surface. The amount of oxide phase was determined from the cathodic polarization curves upon immersing the samples into a corrosive medium. The cathodic polarization curves in NaCl and NaHCO₃ media are presented in Figs. 3 and 4. The oxide film reduction process is accompanied by the hydrogen reduction reaction, therefore, the baseline for oxide film reduction was created and the obtained area was integrated. The sample polarization resistance was measured before this test. The obtained data are listed in Table 1.

Polarization resistance values of Zn–Ni alloy in NaCl solution show an evident tendency to reduce with increasing the immersion time, while the amount of the oxide, which forms on the sample surface increases at the same time. The reduction of R_p values was not observed in NaHCO₃ media, besides, it can be seen from the data presented in Table 1 that the thickness of the oxide film formed in this solution is significantly less than in NaCl.

Dissolution products

Zn and Ni concentrations were determined after a corrosion attack by a direct current plasma emission spectroscopy in the test solution and in the corrosion product film as well. The measurements were carried out after different immersion periods at the open circuit potential in the test media and under potentiostatic polarization at the anodic potentials. The obtained results are presented in Fig. 5 and are listed in Table 2.

The total amount of corroded metals consists of the parts dissolved in the test media and of that one which has passed into the film. This total amount appeared to be dependent on the test media and in general was higher for the nearly neutral NaCl solution in comparison with alkaline NaHCO₃. Variations in the amount of the corroded metals in different media became evident starting from 48 h of sample exposure. The Zn concentration in the chloride solution was found to be higher than the

Table 1. Polarization resistance (R_p) and charge used for oxide film reduction (Q)

	Immersion in NaCl solution				Immersion in NaHCO ₃ solution			
	0 h	24 h	48 h	72 h	0 h	24 h	48 h	72 h
R_p , Ω	1457	1480	1030	851	1110	2070	1187	–
Q , μC	3.7	45.3	58.7	72.3	2.1	5.2	12	10

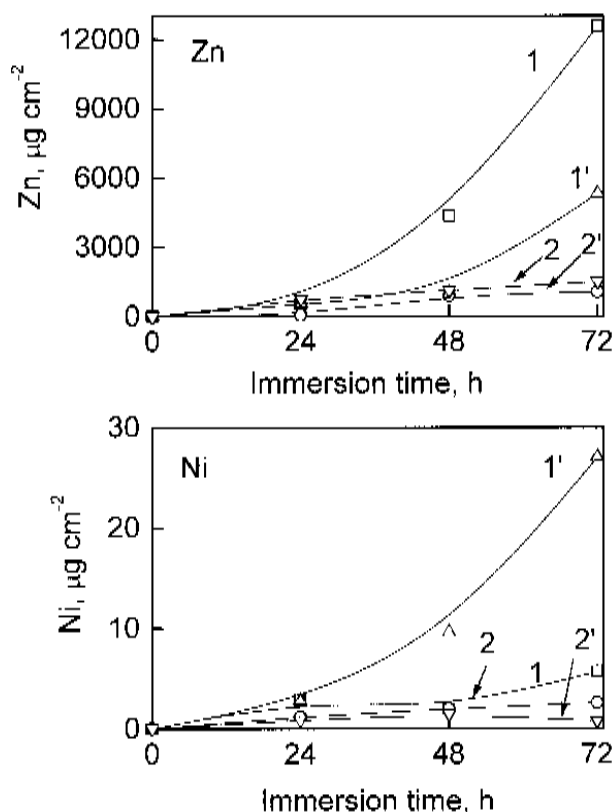


Fig. 5. Amount of dissolved Zn and Ni in NaCl (1, 1') and NaHCO₃ (2, 2') test media. 1, 2 – in the solution, 1', 2' – in the film

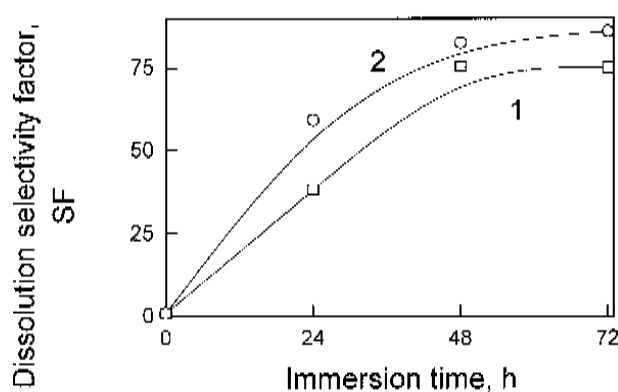


Fig. 6. Dissolution selectivity factors of Zn–Ni samples at the corrosion potential in NaCl and NaHCO₃ solutions

where N_{Zn}^{2+} and N_{Ni}^{2+} are the total amounts of Zn and Ni in moles, determined in the test solution and the film, and N_{Ni} , N_{Zn} are the mole fractions of Zn and Ni in the alloy. The calculated Zn–Ni alloy dissolution selectivity factors are presented in Fig. 6.

SF values were found to increase with an increase of the immersion time up to 48 h with the following stabilization. In general, SF rates were slightly higher for NaHCO₃ ambient.

The highest amount of corroded metals was detected when the film did not appear on the alloy surface, *i.e.* in (NH₄)₂SO₄ solution. The SF values

Table 2. The amounts of Zn and Ni dissolved in solutions and passed to the corrosion product film under potentiostatic polarization and the selective dissolution factors (SF) of Zn–Ni electrode in NaCl, NaHCO₃ and (NH₄)₂SO₄ solutions

Polar. cond.	Test site	NaCl			NaHCO ₃			(NH ₄) ₂ SO ₄		
		Zn, µg	Ni, µg	SF	Zn, µg	Ni, µg	SF	Zn, µg	Ni, µg	SF
a	sol.	14.45	0.065	31.2	1.04	0.35	5.24	18.4	0.03	77.1
	cor. pr.	0.54	0.04		0.23	0.06		–	–	
b	sol.	52.8	0.2	19.1	7.4	0.22	3.54	65.6	0.12	74.3
	cor. pr.	1.65	0.02		2.8	0.04		–	–	

Zn amount detected in the film, while for HCO₃[–] solution these two parts of corroded Zn were similar (Fig. 5, curves 2 and 2'). Meanwhile, the distribution of the corroded Ni between the solution and the film differs from the Zn case, especially in the Cl[–] media. The main part of corroded Ni was detected, contrary to Zn, in the hardly soluble corrosion products (Fig. 5, curves 1 and 1').

The dealloying process can be characterized by the dissolution selectivity factor (SF), which can be found by the analysis of the corrosion environment [8]:

$$SF = \frac{N_{Zn}^{2+} \cdot N_{Ni}}{N_{Ni}^{2+} \cdot N_{Zn}} \quad (1)$$

were determined to be highest in this medium as well, meanwhile, the lowest dissolution rates and the lower selectivity factors for Zn–Ni alloy corrosion were observed in NaHCO₃ solution.

Surface analysis

Investigations of element concentration on the surface of the initial Zn–Ni samples and after the corrosion attack was carried out by means of energy dispersive X-ray analysis (EDXA). The obtained spectra are presented in Fig. 7.

The presence of Zn and Ni lines was observed in the corresponding spectra, while their intensity, diminished after a surface corrosion attack. It may be caused by the presence of a film. Information on

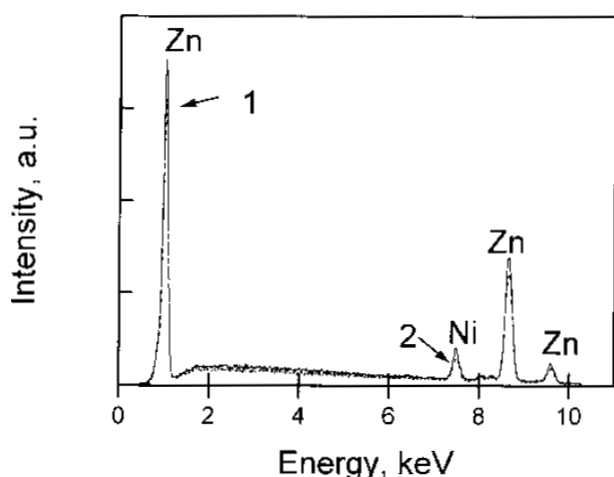


Fig.7. EDXA spectra of the initial (1) and after corrosion attack (2) Zn–Ni sample in NaCl solution at corrosion potential for 24 h

the element concentration obtained with EDAX technique is gained from ~1 μm, hence it is not very suitable to study strictly superficial phenomena.

X-ray diffraction studies

Selective dissolution of metals from intermetallic structures in addition to the formation of a more noble metal-enriched non-equilibrium surface should enrich its surface with structural defects [19]. X-ray diffraction line broadening is recognized to be caused by crystallite size and lattice strains [20–22]. In general, the grain size of Zn electrodeposits lies in the range of 0.1–10 μm and X-ray diffraction is quite insensitive to its variations [23, 24], so the observed line broadening will be caused mostly by lattice imperfections.

X-ray diffractograms of the initial Zn–Ni sample and after the corrosion attack are presented in Fig. 8.

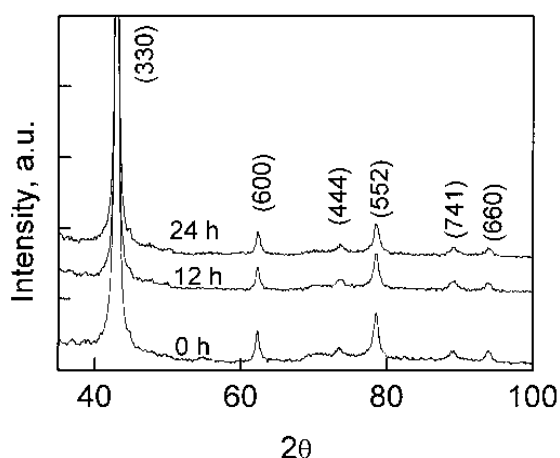


Fig. 8. XRD patterns of Zn–Ni alloy samples after different time of corrosion attack in NaCl solution

Plane (hkl)	Integral breadth after corrosion test		
	0 h	24 h	48 h
(330)	0.381	0.398	0.429
(552)	0.807	0.865	0.999
(741)	1.353	1.225	1.321
(660)	0.678	0.793	0.844

The integral breadth of the diffraction lines was determined, and the obtained results are listed in Table 3. An increase in the diffraction line integral breadth for the samples exposed to corrosion tests can be observed. Besides, an increase in this parameter is more significant for a longer exposure to the test media. The obtained data show that the Zn–Ni corrosion process in NaCl solution is accompanied by the formation of a more distorted metal phase lattice.

Surface analysis of the metal phase

Surface analysis of the samples exposed to corrosion attack was carried out by X-ray photoelectron spectroscopy (XPS). Zn 2p_{3/2}, Ni 2p_{3/2}, O 1s, C 1s, Cl 1s and Na 1s lines were analyzed and the surface concentration of the principal alloy components was determined after a soft surface sputtering. The criterion to stop surface cleaning was the moment when the carbon, chlorine and sodium intensities were close to zero. The obtained results on Zn, Ni and O concentrations are shown in Table 4.

It appeared impossible to obtain reasonable XPS results for a more prolonged exposure time (72 h), possibly because of significant corrosion damages and the resulting surface roughening. Nevertheless, an increase of Ni concentration on the corroded Zn–Ni samples can be observed. Therefore, it can be stated that a Ni-enriched surface layer formation during Zn–Ni alloy corrosion takes place.

The properties of such layers and their influence on the corrosion behaviour of the alloy will be the subject of the future investigations.

Exposure time, h	Zn, at. %	Ni, at. %	O, at. %
0	90.2	4.1	5.6
24	89.5	5.9	4.5
48	85.4	7.5	7.1

CONCLUSIONS

Selective dissolution of Zn–Ni alloy takes place in NaCl, NaHCO₃ and (NH₄)₂SO₄ solutions at the open circuit potentials, as well in the anodic potential region. The highest values of the dissolution selectivity factor for polarized electrodes were determined in (NH₄)₂SO₄ and the lowest in NaHCO₃ media.

Selective corrosion of Zn–Ni alloy causes:

1. A decrease of the anodic Tafel constants in the case of electrode polarization in NaCl solution.

2. An increase of the diffraction line integral breadth, what implies the formation of a more distorted lattice.

3. The formation of a Ni-enriched surface layer.

The corrosion product film which forms on Zn–Ni surface in NaCl solution – is thicker in comparison with that one which forms in a NaHCO₃ medium.

Received 31 January 2001

Accepted 5 February 2001

References

- R. Ramanauskas, P. Quintana, P. Bartolo-Perez and L. Diaz-Ballote, *Corrosion*, **56**, 588 (2000).
- H. Leidheiser Jr and J. Suzuki, *J. Electrochem. Soc.*, **128**, 242 (1981).
- J. R. Vilche, K. Jüttner, W. J. Lorenz, W. Kautek, W. Paatsch, M. H. Dean and H. Stimming, *J. Electrochem. Soc.*, **136**, 3773 (1989).
- R. Ramanauskas, *Appl. Surf. Sci.*, **153**, 53 (1999).
- N. R. Short, A. Abibsi and J. K. Dennis, *Trans. Inst. Met. Fin.*, **67**, 73 (1989).
- G. W. Loar, K. R. Romer and T. J. Aol, *Plat. Surf. Fin.*, **78**, 74 (1991).
- M. Stein, S. P. Ovens, H. W. Pickering and K. G. Weil, *Electrochim. Acta*, **43**, 223 (1998).
- I. D. Zartsyn, I. V. Protasova, A. E. Shugurov and I. K. Marshakov, *Prot. Metals*, **32**, 429 (1996).
- H. Kaiser, *Materials and Corrosion*, **47**, 34 (1996).
- J. Morales, P. Esparza, S. Gonzalez, L. Vazquez, R. C. Salvarezza and A. J. Arvia, *Langmuir*, **12**, 500 (1996).
- K. Sieradzki, *J. Electrochem. Soc.*, **140**, 2868 (1993).
- R. Ramanauskas, L. Muleshkova, L. Maldonado and P. Dobrovolskis, *Corros. Sci.*, **40**, 402 (1998).
- R. Ramanauskas, P. Quintana, L. Maldonado, R. Pomes and M. A. Pech-Canul, *Surf. Coat. Tech.*, **92**, 16 (1997).
- H. W. Pickering, *Corros. Sci.*, **23**, 1107 (1983).
- D. Abayarathna, E. B. Hale, T. J. O'Keefe, Y.-M. Wang and D. Radovic, *Corros. Sci.*, **32**, 755 (1991).
- T. E. Graedel, *J. Electrochem. Soc.*, **136**, 193C (1989).
- R. Guo, F. Weinberg and D. Tromans, *Corrosion*, **51**, 356 (1995).
- K. R. Baldwin, M. J. Robinson and C. J. E. Smith, *Corros. Sci.*, **35**, 1267 (1993).
- K. E. Heusler, *Corros. Sci.*, **39**, 1177 (1997).
- Th. H. De Keijser, J. I. Langford, E. J. Mittemeijer and A. B. P. Vogels, *J. Appl. Cryst.*, **15**, 308 (1982).
- S. Enzo, G. Fagherazzi, A. Benedetti and J. Polizzi, *J. Appl. Cryst.*, **21**, 536 (1988).
- D. J. Balzar, *J. Appl. Cryst.*, **25**, 559 (1992).
- B. D. Cullity, *Elements of X-Ray Diffraction*, 2nd ed., p. 285, Addison-Wesley, Reading USA (1978).
- J. G. M. Van Berkum, R. Delhez, Th. H. de Keijser and E. J. Mittemeijer, *Acta Cryst.* **A52**, 730 (1996).

E. Ivaškevič, A. Selskis, A. Sudavičius,
R. Ramanauskas

ELEKTROLITINIŲ CINKAS-NIKELIS LYDINIO DANGŲ DECINKACIJA

S a n t r a u k a

Elektrolitinio Zn–Ni lydinio atrankinis tirpimas NaCl, NaHCO₃ ir (NH₄)₂SO₄ tirpaluose buvo tiriamas atviros grandinės sąlygomis ir anodinių potencialų srityje. Aukščiausios tirpimo atrankumo faktoriaus reikšmės poliarizuotiems elektrodams buvo nustatytos (NH₄)₂SO₄ tirpale, o žemiausios – NaHCO₃ terpėje. Zn–Ni lydinio atrankinė korozija lydi nikelio prisodrinto paviršinio sluoksnio susidarymas.

Dėl šios priežasties sumažėja anodinės Tafelio konstantos, kai elektrodas poliarizuojamas NaCl tirpale, ir išauga difrakcinės linijos integralinio pločio reikšmės, o tai rodo, kad susidaro labiau iškreipta metalo gardelė. Nustatyta, kad korozijos produktas – susidariusi NaCl tirpale ant Zn–Ni paviršiaus plėvelė yra storesnė negu plėvelė, susidariusi NaHCO₃ terpėje.

Э. Ивашкевич, А. Сельскис, А. Судавичюс,
Р. Раманаускас

ОБЕСЦИНКОВАНИЕ ПОКРЫТИЙ ИЗ ЭЛЕКТРОЛИТИЧЕСКОГО СПЛАВА Zn–Ni

Р е з ю м е

Селективное растворение электролитического сплава Zn–Ni исследовали в условиях отсутствия поляризации, а также в области анодных потенциалов. Наиболее высокие значения фактора селективности растворения для поляризованных электродов были определены в (NH₄)₂SO₄ растворе, а наименьшие – в NaHCO₃ среде. Селективная коррозия сплава Zn–Ni сопровождается образованием обогащенного никелем поверхностного слоя.

В результате этого уменьшаются анодные Тафелевские константы при поляризации электрода в NaCl растворе и увеличиваются значения интегральной ширины дифракционной линии, что указывает на образование более искаженной ячейки металла.

Определено, что продукт коррозии – образовавшаяся пленка на Zn–Ni поверхности в NaCl растворе является более толстой, чем пленка, образовавшаяся в NaHCO₃ среде.